Chemical Vapor Deposition

DOI: 10.1002/cvde.201300054

Review

Modification and Resonance Tuning of Optical Microcavities by Atomic Layer Deposition**

By *Jiao Wang, Gaoshan Huang,* and *Yongfeng Mei**

Recently, enormous interest has been focused on the nanofabrication of optical micro- and nanocavities for applications in lab-on-a-chip and quantum optics. At the same time, the atomic layer deposition (ALD) process presents several advantages for the fabrication and modification of micro- and nanostructures because of its atomic level thickness fine-tuning and perfect coating conformability in three-dimensional (3D) structures. Hence, ALD technology has been directed into the field of optical microcavities for the tracking and tuning of their properties. In this short review, we will summarize recent progress in the application of ALD on optical microcavities. Firstly, we will briefly introduce ALD technology and emphasize its distinctive features when applied to optical microcavities. Then, various microcavities such as photonic crystals, opals, and tubular microcavities will be illustrated to demonstrate their development with the assistance of ALD technology. Such an influential manufacturing tool for optical devices could inspire numerous interesting applications, as concluded in the final part.

Keywords: ALD, Optical microcavity, Photonic crystal, Plasmonic nanocavity, Rolled-up micro-tube

1. Introduction

Since its development in the 1970 s,[1] ALD has been an effective method of thin film deposition, and has proven suitable for producing large-size thin films of a high quality.[2] ALD has several advantages, including thickness control on the atomic scale, production of highly conformal films, low temperature growth, and wide-area uniformity.[2] Generally, ALD is becoming an important thin film deposition method for nanotechnology, and is used to fabricate thin film coatings on complex microstructures such as 3D photonic crystals,[3,4] electrospinning polymer films,[5] and many others. The applications extend from planar-type thin film deposition to pore-size tuning,[6,7] optical tuning, catalysis,[5] Li-ion batteries,[8,9] and more. Currently, in addition to the traditional metal,[10–12] oxide,[13,14] semiconductor,[15–18] and nitride[19–21] thin layers, various thin films with special physical properties, such as up-/down-conversion luminescent properties,[22,23] can also be obtained via the ALD procedure.

Recently, ALD has attracted the attention of researchers in the field of micro-/nanodevices.[24] The precise control of the deposited layer thickness allows for new strategies in the modification of the chemical and physical properties of micrometer-/nanometer-scaled materials or micro-/nanodevices. The promising applications in the field of optical microdevices are gaining special attention.[25,26] Besides the deposition of functional thin films, the unique potential of ALD for modifying nanostructured materials or microdevices is now widely appreciated. During the past ten years, the ALD procedure has been used for the fabrication or design of new optical devices. Generally, modifying optical properties via surface coating has been used as one effective method for modifying the properties and applications of optical microdevices. Post-fabrication tuning of the resonant azimuthal modes of silicon optical microcavities (photonic crystal or self-rolled tubular microcavities) can be achieved via ALD methods.[25]

This review focuses on the new and emerging applications of ALD in optical microcavities. Various microcavities such as photonic crystals, opals, tubular microcavities, and plasmonic nanocavities will be illustrated to demonstrate their development under the assistance of ALD technology. As an effective manufacturing tool for optical microdevices,

[*] Dr. J. Wang, Prof. G. S. Huang, Prof. Y. F. Mei
Department of Materials Science, Fudan University, Shanghai 200433 (P. R. China)
E-mail: yfm@fudan.edu.cn

[**] This work is supported by the Natural Science Foundation of China (Nos. 51322201, 51102049 and 51302039), "Shu Guang" project by Shanghai Municipal Education Commission and Shanghai Education Development Foundation, Project Based Personnel Exchange Program with CSC and DAAD, Specialized Research Fund for the Doctoral Program of Higher Education (No. 20120071110025), and Science and Technology Commission of Shanghai Municipality (No. 12520706300).

 © 2014 WILEY-VCH Verlag GmbH & Co. KGaA, Weinheim

ALD could inspire numerous interesting applications in the fields of bio-inspired devices, optical microcavities, and bio-/chemical sensors.

2. Characteristics of ALD as One Tool for the Fabrication of Optical Microcavities

Optical microcavities confine light to small volumes by resonant recirculation, however all optical microcavities exhibit light loss at a certain level. As one example, whisper-gallery-mode (WGM) resonators are typically dielectric spherical structures in which light waves are confined by continuous total internal reflections. The light travelling in the WGM microcavities relies on the principle of total internal reflection at the interface between high refractive index materials and low refractive index materials. Each reflection involves a loss of a few percent of the light intensity, usually due to absorption by the material of the microcavity and the surface roughness.[27,28] The quality of optical microcavities is limited by this light loss. Thus, surface roughness, conformality, and homogeneity of the sensor material are very important factors to consider when trying to obtain high-performance optical micro-devices.[27,28] For novel optical microcavity research, the controllable layer thickness and composition, as well as the ability to conformally coat complex 3D structures, are essential characteristics.

To this end, thin film deposition techniques for optical microdevice modification should provide: (1) Excellent conformality in nanometer-scale complex structures with very high aspect ratios; (2) very good uniformity over a large scale with a smooth surface; (3) good precursor material properties with minimum damage to the substrate materials or geometries; and (4) the growth temperature low enough for future processes. As one vapor-phase thin film deposition technique, ALD technology undoubtedly fulfills all of these requirements. The typical ALD process includes four steps (Fig. 1).[2,24,29] (1) Metal-containing precursor exposure, (2) evacuation or purging of the precursors and any by-products from the chamber, (3) exposure of the other reactant species (non-metal-containing precursor), (4) evacuation or purging of the reactants and by-product molecules from the chamber. ALD allows atomic layer-by-layer deposition with nearly 100% step coverage. Thus highly conformal films with excellent uniformity and thickness control can be deposited not only on flat surfaces, but also inside trenches and narrow openings via the facile ALD technique at low deposition temperatures (50–400 °C). This method can also introduce new chemical and physical properties in various 3D complex structures for novel applications, such as luminescent properties,[30,31] high refractive index contrast,[30,32] and catalysis.[5]

2.1. Low Deposition Temperatures (50–400 °C)

One important advantage of ALD is the ability to deposit high-quality thin films at low deposition temperatures

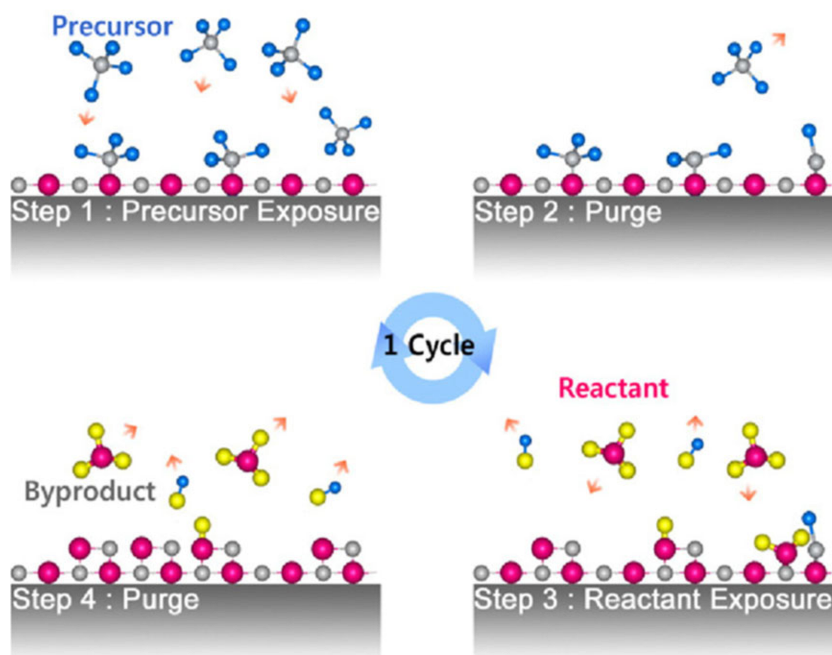

Fig. 1. Schematic of an ALD procedure. One ALD cycle consists of four separate steps. Step 1: the substrate is exposed to precursor 1. Step 2: the excess of precursor 1 and any byproducts in the gas phase are removed by inert gas purging. Step 3: the substrate is exposed to reactant which reacts with the adsorbed precursor 1 to form a layer of the desired material. Step 4: evacuation or purging of the reactants and byproduct molecules from the chamber. This cycle is repeated until the desired thickness of the deposit is reached. (Reproduced with permission.[24] Copyright 2009, Elsevier B.V.)

 © 2014 WILEY-VCH Verlag GmbH & Co. KGaA, Weinheim

(50–400 °C). In typical ALD procedures (Fig. 1),[2,24,29] thermal activation of the adsorption and reaction of precursor molecules on the substrate surface is necessary. Thus, heat treatment is required for thin film deposition via ALD methods. Depending on the precursor conditions, the substrate materials, and the density and crystallinity of the final thin films, it is possible to deposit pure thin films in the temperature range 50 °C to 400 °C. The ability to grow thin films at low deposition temperatures is extremely useful for coating heat-sensitive materials such as polymers[5,33–35] and biomaterials,[36,37] and heat-sensitive structures such as self-rolled microtubes with (ultra-)thin wall thickness.[38] For the design and modification of optical micro-/nanodevices, low deposition temperature ALD is promising to be one effective method.

2.2. Atomic Level Control of Layer Thickness and Composition

For the optical micro-/nanodevices, light loss is normally caused by the rough surface.[27,28] The ability to construct compositionally modulated thin films is very important for the design and application of optical micro-/nanodevices. As one technique used to deposit thin atomic films layer-by-layer at atomic level, ALD can be used to deposit thin smooth films with precisely controlled thickness and controllable composition (Fig. 2). Normally, because the actual deposition thickness per cycle is often a small fraction of one molecular layer for many materials,[9,41,42] the thin films deposited via ALD technology are of high density and without pin holes (roughness < 1 nm).

ALD is undoubtedly an effective and facile method for forming low light-loss thin films on complex 3D optical micro-/nanostructures. The 2D slab photonic crystal could be conformally coated with amorphous TiO_2 by ALD step-by-step (Fig. 2a, 20–120 nm).[39] The X-ray nanolaminates with smooth interface also can be obtained via this method (Fig. 2b),[40] however, compared to virtually all other deposition techniques, the growth rate of ALD is very low.

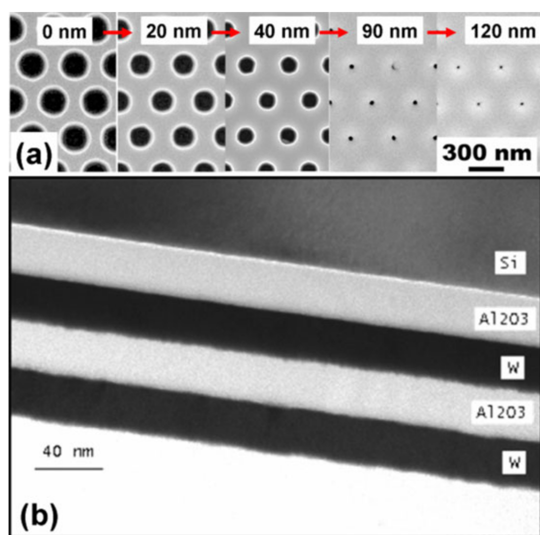

Fig. 2. a) Top-view SEM images of a triangular lattice Si slab PC coated with various TiO_2 ALD thicknesses (0–120 nm) (Reproduced with permission.[39] Copyright 2006, American Institute of Physics). b) TEM image of a two-bilayer W/Al_2O_3 nanolaminate grown at 177 °C (Reproduced with permission.[40] Copyright 2006, American Chemical Society).

In the early days of its development, ALD was limited to the deposition of epitaxial layers of II–VI or III–V semiconductors. With the development of fabrication technology, ALD has found new applications in depositing polymer and inorganic composite materials with smooth surface and interface (Fig. 2).[39,40,43,44] Recently, ALD was used to successfully synthesize rare earth-doped (up-conversion) luminescent nanometer-scale thin films, including Er-doped Al_2O_3,[45] Er-doped Y_2O_3,[22] and rare earth-doped HfO_2.[46] Highly conductive and transparent hybrid organic/inorganic thin films have been grown using ALD techniques.[47] For the design and modification of optical devices, high refractive index oxide and semiconductor materials can also be deposited via ALD, including Al_2O_3,[12] TiO_2,[4,48] HfO_2,[49–51] GaAs,[52,53] Ta_3N_5,[54,55] ZnS,[31] and so on. For self-rolled optical microcavities with ultra-thin wall and polymer (PS spheres) photonic crystals, all these materials are good candidates with high refractive index for surface modification and mode controlling.

2.3. Conformal Coating Ability for Complex 3D Structures

ALD is a cyclic process which relies on the sequential self-terminating reactions between gas-phase precursor molecules and a solid surface. The unique self-limiting nature of this chemical reaction process gives better thickness control, conformality, film quality, and thickness uniformity on 3D structures with large aspect ratios than other deposition techniques.[56] The excellent conformality of ALD is a highly useful feature for many applications in optical micro-/nanodevices with complex 3D structures, such as photonic crystals, opals, and tubular optical microcavities.[27,28] Its large area conformality is especially good for the surface modification of optical microdevices or systems.

Figure 3 shows a collection of complex micro-/nanostructures synthesized via the ALD approach. Within the accuracy of the images (Fig. 3a), a perfect 100% conformal Al_2O_3 coating has been achieved in all the trenches on a Si wafer.[57] Highly ordered nanotube arrays, possessing uniformity over a large area, can be achieved using microporous silicon templates and ALD techniques (Fig. 3b).[58] Anodic aluminum oxide (AAO) is one effective and often-used template for the fabrication of complex 3D nanostructures.[12,59,63–65] The resultant silica-coated commercial AAO membranes with specific surface chemistry and controlled pore size are applicable for advanced molecular separation, cell culture, tissue engineering, biosensing, and drug delivery.[64] Nested multiple-walled

© 2014 WILEY-VCH Verlag GmbH & Co. KGaA, Weinheim

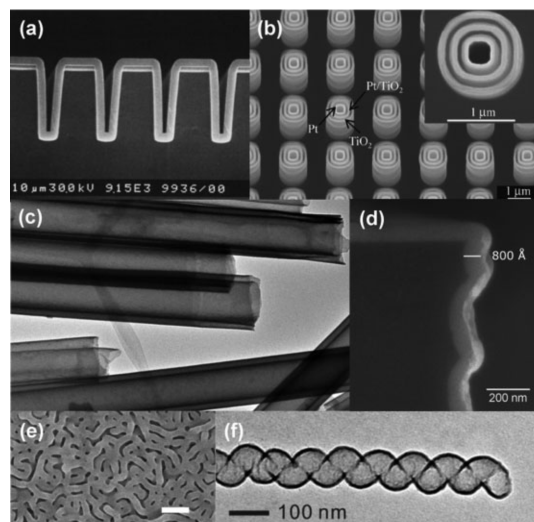

Fig. 3. Complex micro-/nanostructures synthesized by ALD: a) Cross-sectional SEM image of an Al_2O_3 ALD film with a thickness of 300 nm on a Si wafer with a trench structure (Reproduced with permission.[57] Copyright 1999, WILEY-VCH Verlag GmbH). b) Highly ordered arrays of nested semiconductor/metal nanotubes (Reproduced with permission.[58] Copyright 2011, Springer). c) TEM image of several chemically released and separated coaxial HfO_2 nanotubes (Reproduced with permission.[59] Copyright 2010, American Chemical Society). d) SEM image of top corner of a trench with a 800 Å Ga_2O_3 film deposited onto high-aspect-ratiosilicon trenches to assess the conformality of the ALD process (Reproduced with permission.[60] Copyright 2012, American Chemical Society). e) SEM images of the alumina-coated BCP templates subjected to 10 cycles (Reproduced with permission.[61] Copyright 2012, American Chemical Society). f) TEM images of helical Al_2O_3 nanotubes obtained by applying 50 cycles of Al_2O_3 deposition (Reproduced with permission.[62] Copyright 2010, WILEY-VCH Verlag GmbH).

coaxial nanotube structures of transition metal oxides, semiconductors, and metals were also successfully synthesized by ALD techniques utilizing nanoporous AAO as templates (Fig. 3c).[59] Figure 3d shows an scanning electron microscopy (SEM) image of the top corner of a trench with 800 Å Ga_2O_3 film deposited onto high-aspect ratio silicon trenches to assess the conformality of the ALD process.[60] Mesoporous metal oxide networks composed of interconnected nanotubes with finely tunable ultrathin tube walls down to 3 nm, and high porosity up to 90%, were fabricated by ALD of alumina or titania onto templates of swelling-induced porous block copolymers (BCP) (Fig. 3e).[61] Transmission electron microscopy (TEM) images indicated that the helical Al_2O_3 nanotubes (Fig. 3f) were obtained by applying 50 cycles of Al_2O_3 ALD deposition onto carbon nanocoils used as sacrificial templates.[62] The perfectly replicated helical morphology of the initial carbon nanocoil templates highlights the advantage of ALD for the coating of high-curvature surfaces.[62,66] Meanwhile, photocatalytic polymer/inorganic core/shell nanofibers were produced via a two-step approach (electrospinning and ALD processes).[5] These interesting examples highlight the versatility and particular suitability of ALD for the fabrication of complex 3D micro-/nanostructures.

ALD is already one effective technology for fine-tuning the surface properties and diameters of the pore size of 2D and 3D optical microcavities. Several researchers have used this effective technique to fabricate high-performance multilayer 3D photonic crystals from synthetic silica opals and holographically patterned polymer templates to control the photonic band properties of photonic crystals for further potential applications in the field of optical microdevices. In the following section, we will focus on the development of ALD with respect to applications in the field of optical microcavities.

3. Development of ALD in the Field of Optical Microcavities

Several methods have been used to modify the optical properties of optical microcavities or microdevices, such as choosing high refractive index materials, adding surface coatings, and injecting luminescent nanoparticles/microfluidics. As mentioned in the previous section, for typical polymer or colloid nanostructures, low-temperature ALD technology is highly suitable for the fabrication of opals or for the tuning of optical properties, due to ALD producing great conformation on these complex 3D structures. For various different kinds of materials, including semiconductors or metal oxides possessing a high refractive index or luminescent properties, the optical properties of optical devices can be tuned over a wide range. Furthermore, multilayer coating and doping of thin film structures can be performed in a highly controllable manner. Surface engineering by ALD on nanowires/nanotubes, devices, and chemical patterns has a potential application in high-performance optical micro-/nanodevices. Currently, the application of ALD for optical devices is one of the most active development fields for fabrication and modification of novel optical microdevices. Several research groups have employed the ALD method for the coating or modification of synthetic opals, other 3D photonic crystals, or self-rolled tubular optical microcavities. In this section, we will discuss the development of ALD in the field of optical microcavities, choosing three kinds of optical microcavities–photonic crystals, tubular optical microresonators, and plasmonic nanocavities–as the main discussion subject. Some other optical microdevices will also be briefly introduced.

3.1. Photonic Crystals and Opals

Since 2003,[67] photonic crystals have been intensively investigated for their potential to confine, as well as to guide, light. Many researchers have demonstrated that ALD allows rapid and flexible fabrication of photonic crystals,[39,53,68–71] and opals.[4,31,52,72,73]

Normally, photonic crystals are formed by self-assembly of polymer or silica nano-/microspheres. ALD has been used to create inverted replicas of holographically defined photonic crystal, followed by removal of the polymeric or

 © 2014 WILEY-VCH Verlag GmbH & Co. KGaA, Weinheim

silica template.[69] The ALD approach for self-assembled 3D photonic crystals and opal structures has been extended to include a broad variety of materials. Ta_3N_5,[74] ZnO,[75,76] GaAs,[52,53] Al_2O_3,[71,77] TiO_2,[72,73] and ZnS[31] have all been used to produce multilayer inverse opal structures. The wavelength of the peak Bragg reflection was observed to shift to progressively longer wavelengths versus the ALD thickness of inorganic thin films.[53,72,77] The Bragg peak shifts show a strong relationship with the increase in the effective refractive index of the opal structure as the higher refractive index inorganic films coated on the opal structures. These results demonstrate that the location and intensity of the Bragg peak from photonic crystals can be tuned using ALD. The most typical example is the research on a TiO_2-based 3D photonic crystal (Figs. 4a and b).[73] Figure 4b is an intensity plot of wavelength versus ALD cycles, after interpolation, clearly showing a shift in the pseudo-photonic bandgap (PPBG) peaks.[73] The optical spectra of this photonic crystal can be tuned over a wide range by varying the number of ALD cycles (Fig. 4b).[73] Following this interesting research, one additional sacrificial layer of ZnS or Al_2O_3 was deposited via ALD on the opal structure. This technique provides a reliable method for the fabrication of high-quality, non-close-packed, inverse-shell opals with large static tunability and precise structural control.[78] In addition, this method will allow the facile fabrication of 3D photonic crystals with optimized photonic bandgaps, which could enhance the variation in the optical properties of the TiO_2 photonic crystal.[78] ALD has been demonstrated to be beneficial in the control of the propagation of light via back reflections, slow photons, and surface-resonant modes in these 3D inverse opals. As such, these 3D inverse opals are promising for the application in dye-sensitized solar cells,[79] photocatalysis, water splitting,[80] and up-conversion luminescence.[81]

2D slab photonic crystals are being actively investigated because of their many unique properties, i.e., submicron beam control, self-collimation, superprism effects, negative refraction, and the ability to control the speed of light.[71,82] All of these interesting optical properties are dependent on the precise control of dielectric material, however the optical properties of these 2D slab photonic crystals show limited post-fabrication tunability. Following the fabrication and modification of high-quality 3D photonic crystals via ALD, this process has become one powerful tool in the field of 2D photonic crystals.[39,68,82,83] In the first published paper about 2D photonic crystals, one 2D array of ZnO nanowires was coated with a thick TiO_2 layer and interconnections were formed between the vertically aligned and close-packed ZnO nanowires.[68] Then, the ALD technique was applied to silicon/TiO_2 composite 2D photonic crystal slab waveguides, and the progressive coating, and resulting air hole size reduction was shown to yield precise static tuning of

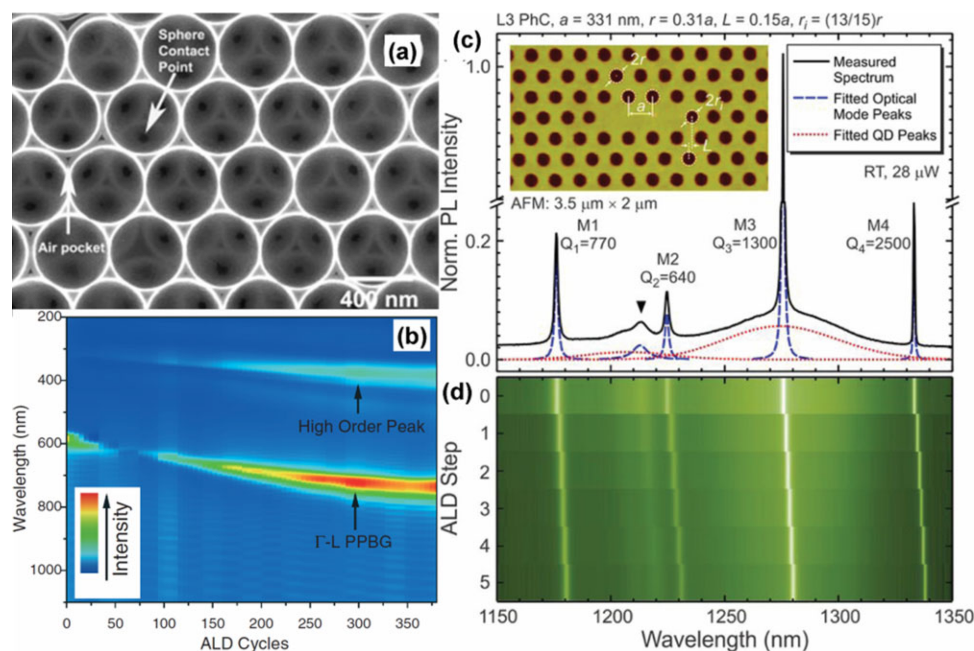

Fig. 4. a) SEM image of 433 nm TiO_2 inverse opal: ion-milled surface. b) Reflectivity data from stepwise TiO_2-infiltrated 266 nm SiO_2 opal. Interpolated intensity plot of wavelength versus ALD cycles, indicating the position of Γ-L PPBGs. Regions of high reflectivity are indicated by arrows (Reproduced with permission.[73] Copyright 2005, WILEY-VCH Verlag GmbH & Co. KGaA, Weinheim). c) Room temperature μ-PL spectrum of as-processed L3 GaAs Photonic crystal nanocavity. The blue dashed lines are individual fitted optical mode spectra (M1–M4). One broad mode at 1213 nm is marked by a solid triangle but is not labeled. The red dotted lines are fitted QD-related peaks. The inset is a 3.5 μm × 2 μm atomic force microscopy (AFM) image ofthe cavity after five ALD steps with relevant structural parameters. d) Color-coded μ-PL intensity map showing the mode peaks as a function of ALD step. One ALD step corresponds to 0.9 nm Al_2O_3 coating (Reproduced with permission.[71] Copyright 2011, American Institute of Physics).

the photonic band structure.[39] Subsequently, the frequency and dispersion of photonic bands in 2D triangular-based superlattice photonic crystal Si slab waveguides were manipulated using ALD.[82] More recently, researchers have experimentally investigated the effect of ALD on tuning optical modes in GaAs L3 photonic crystal air-bridge cavities (Fig. 4c inset).[71] Four distinct optical mode peaks are observed in the photonic bandgap and they show different wavelength-redshifts (0–6.5 nm) as the photonic crystal surface is coated with an Al_2O_3 layer (0–5.4 nm thick) (Fig. 4d).[71] Figure 4c shows a normalized room-temperature photoluminescence (PL) spectrum of an L3 photonic crystal prior to ALD coating.[71] Figure 4d shows color-coded PL spectra as functions of the ALD deposition step. This experimental result shows a clear redshift of all optical modes with the ALD step increasing, which fits well with the finite-difference time-domain (FDTD) simulation.[71]

3.2. Microcavities with Tubular Geometry

Besides photonic crystals and opals, tubular optical microcavities with WGMs also show special applications in various fields, including bio-/chemical sensors, cell culture, opto-microfluidics, microlaser, and thermometry. The tunable optical properties are also desirable for these tubular optical microresonators. Based on the experimental and calculated results, it is noticeable that ALD presents one promising way to tune the optical mode of rolled-up optical microcavities with tubular geometry with varying wall thickness.[84,85] Figure 5a shows a schematic cross-section diagram of an SiO/SiO_2 microtube before and after ALD coating with Al_2O_3 which indicates that the deposited material is coated on both the inner and outer surfaces of the tube.[84] Figure 5b shows a series of PL spectra for the microtube with Al_2O_3 coatings of up to 100 monolayers (MLs) (the normalized peak intensity is color coded). An average redshift of 33 meV was clearly measured for all modes. The spectral resonator position and polarization of the modes can also be smoothly tuned in a wide spectral range by Al_2O_3 coating, which can be well described by FDTD calculations (Fig. 5c).[84] This process suggests that the microtubes could be used in potential applications for lab-on-a-chip components.

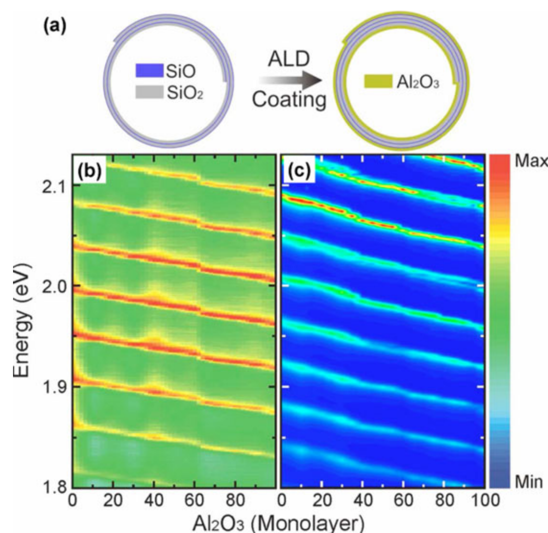

Fig. 5. a) Schematic cross-section diagram of an SiO/SiO_2 microtube before and after ALD coating with Al_2O_3. b) Color-coded normalized peak intensity of PL spectra showing the energy shift for the resonant modes from a microtube of 7 μm in diameter coated with Al_2O_3 up to 100 MLs. c) FDTD simulations for the actual tube in b) for the energy shift of the resonant modesas a function of the number of ML coatings. (Reproduced with permission.[84] Copyright 2009, Optical Society of America)

Based on this research, very thin microtube walls are the cause of the high sensitivity and could be further optimized by adjusting their thickness via ALD. Researchers have also found that ALD could increase the wall thickness and effective refractive index of the wall.[86] Compared to the ALD Al_2O_3 coating, HfO_2 effectively improves the light confinement of these self-rolled microcavities with thin wall thickness since HfO_2 has a higher refractive index.[86] The ALD coating also provided an enhancement of the structural stability of a lab-in-a-tube microsensor for the detection of individual mouse cells in microtube resonator sensors with a HfO_2 coating.[26,87] Even if the material used in the rolling-up process is non-biocompatible, post-processing after roll-up can include an ALD of materials found to be biocompatible to fit future applications as biosensors. Different kinds of cells can be cultured and detected in the self-rolled-up microcavities with ALD coatings, including mouse cells,[87] yeast cells,[88] neuron cells,[89] and HeLa cells.[26,90]

3.3. Plasmonic Nanocavities

Plasmonics – one rapidly emerging subdiscipline of nanophotonics – is coined for a promising new technology that aims to fabricate novel nanodevices for next generation nanometer-scale electronic applications such as lab-on-a-chip.[91,92] The diffraction of classical optics constrains the size of dielectric photonics, whereas plasmonic devices are only limited in their size by the dimensions of the input/output coupler and the transmitting medium. Surface plasmon polaritons (SPPs) are electron density waves excited at the interfaces between metals and dielectric materials. For researchers in the field of optics, highly localized electromagnetic fields of SPPs may be used to help to concentrate and channel light using sub wavelength structures.[91,92] This could lead to miniaturized photonic circuits with length scales much smaller than those currently achieved.[93] Plasmonics can serve as a bridge between photonics and nanoelectronics. Parallel to the development of plasmonic structures based on metal nanoparticles, the propagation of plasmons along metal waveguides is also being investigated. Currently, plasmonic nanocavity is one attractive and rapidly growing

 © 2014 WILEY-VCH Verlag GmbH & Co. KGaA, Weinheim

research field. Miyazaki and Kurokawa demonstrated nanometric confinement of visible light in a plasmonic nanocavity where two metal layers were separated by a 3 nm thick SiO_2 layer.[94] Channel plasmon sub wavelength waveguide ring resonators can be used to realize plasmonic components in an integrated optical circuit.[93,95]

Owing to its advantages, including surface modification, optical tuning, and layer-by-layer optical characterization, the versatile ALD technology is finding increased use in the emerging field of plasmonic nanocavity.[96] High-throughput fabrication of metal-dielectric-metal sub-10 nm plasmonic nanogap structures and nanoring cavity arrays can be obtained via the conformal deposition of ultrathin sacrificial layers using effective ALD.[97,98]

Palyakov et al. presented a new method for tuning the plasmon absorption resonance wavelength with nanometer precision anywhere from the visible to the near infrared in post-fabrication by the deposition of a few nanometers of aluminum oxide inside the grooves via ALD.[99] Exquisite control over the resonance position was demonstrated in this study of gold gratings that were tuned in a completely reversible manner from a wavelength of 720 nm up to 860 nm by the ALD growth of a layer of Al_2O_3, a few nanometers thick.[99] Meanwhile, this Al_2O_3 ALD coating also serves as a protective layer for the metal nanocavities.[99]

Metallic optical systems can confine light to deep sub wavelength dimensions. To probe metallic optical cavity confinement, emission spectra of individual cavities could be measured as conformal layers of Al_2O_3 were deposited in $\sim$1.8 nm increments using ALD. Each deposition of Al_2O_3 led to a redshift of the cavity modes. By perturbing the cavity modes with conformal dielectric layers of sub nanometer thickness using ALD, the measured exponential decay length of the modes was found to be less than 5% of the free-space wavelength (λ), and the mode volume to be of the order of $\lambda^3/1000$.[42] These experimental results compare well with values calculated from numerical simulations. The ability to continuously vary the resonances of a metal nanocavity via ALD can be used for metrology and cavity-emitter coupling.

3.4. Sundry Optical Devices

Novel state-of-the-art artificial optical microdevices and naturally optical architectures can be researched using the ALD approach. Figure 6 shows a collection of other interesting novel optical microdevices synthesized via ALD. Nanolaminates, such as Al_2O_3/ZnO (Fig. 6a),[100] Al_2O_3/TiO_2 (Fig. 6b),[101] and W/Al_2O_3 (Fig. 2b)[40,102] can be obtained via ALD. The optical properties of some optical devices are tunable using these nanolaminates, for example, the W/Al_2O_3 nanolaminates show a potential application in X-ray optics.[40,102] Fabry-Perot optical microcavities can be fabricated by breaking the symmetry of a nanolaminate, i.e., introduction of a "defect layer".[103] Thus the ALD technology offers an attractive way of fabricating Fabry-

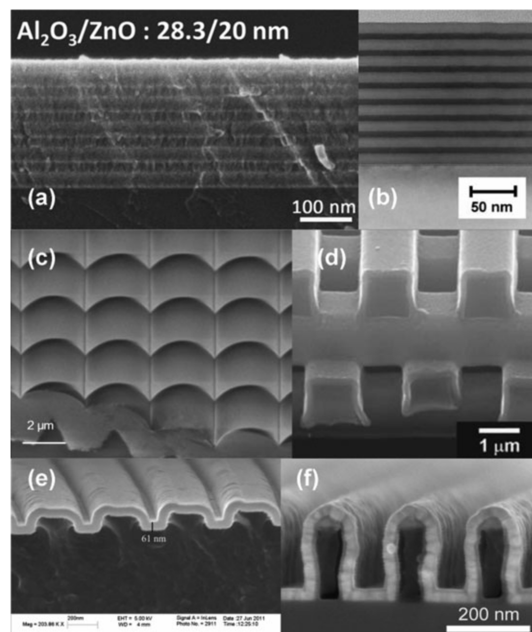

Fig. 6. a) SEM image from a He-ion microscope of nanolaminate cross-sections with Al_2O_3/ZnO bilayer thickness of 48.3 nm (Reproduced with permission.[100] Copyright 2012, American Institute of Physics). b) Cross-sectional TEM image of Al_2O_3/TiO_2 film nanolaminated by alternate ALD growth of 100 cycles Al_2O_3 and 350 cycles TiO_2 (Reproduced with permission.[101] Copyright 2004, Elsevier B.V.). c) Microlens arrays with lens diameterand pitch of 2 μm. The grown material is Al_2O_3 (Reproduced with permission.[105] Copyright 2006, IEEE). d) SEM image of a 4 mm $\times$ 4 mm TiO_2-coated (150 nm) freestanding photonic crystal (side viewat higher magnifications). The periodicity (the distance between rods in each layer) is 2.5 μm (Reproduced with permission.[70] Copyright 2007, American Institute of Physics). e) SEM image of final-cut GMRF sample after TiO_2 coating (61 nm) by ALD (Reproduced with permission.[106] Copyright 2011, Optical Society of America). f) SEM image of the overacted polymer gratingsby ALD (Reproduced with permission.[107] Copyright 2011, Springer).

Perot optical microcavities.[104] The wavelength position and quality of the mode can be tuned by adjusting the thickness and dielectric properties of the defect layer during the multilayer stack ALD. ALD technology can also be used for making optical micrometer and even nanometer- sized lens arrays with 100% fill factor, as shown in Figure 6c.[105] This ALD technology offers a degree of freedom to choose lens materials with a broad range of optical refractive indexes, as well as in controlling the curvature of the lens surface and the fill factor of the lens array for broad applications.[105] Layer-by-layer 3D photonic crystals are fabricated by ALD of a TiO_2 coating on a large size (4 mm $\times$ 4 mm) polymer template created by soft lithography (Fig. 6d).[70] With a highly conformal layer of TiO_2, a significantly enhanced photonic band-gap effect appears at 3.1 μm in transmittance and reflectance (Fig. 6d).[70] The guided-mode resonance filters (GMRF), featuring an amorphous TiO_2 layer fabricated by ALD on a polymeric substrate, are shown in Figure 6e.[106] An iridium wire grid polarizer for UV applications involving a frequency doubling process can be fabricated via an effective multistep process based on ultrafast electron beam lithography and

 © 2014 WILEY-VCH Verlag GmbH & Co. KGaA, Weinheim

ALD.[107] The SEM image of the overacted polymer gratings by the ALD of iridium is shown in Figure 6f.[107] ALD of iridium allows a precise adjustment of the structural parameters of the grating much better than other deposition techniques such as, for example, sputtering. At the target wavelength of 250 nm, a transmission of about 45%, and an extinction ratio of 87, are achieved.[107] Losses in silicon strip and slot waveguides can be reduced with a TiO_2 cover grown via ALD.[108] For waveguides with low effective refractive index n_{eff}, i. e., with a relatively small field confinement, the measured losses stem mostly from leakage through the TiO_2 coating.[108] Highly sensitive GMR sensors for the visible spectral range consist of a silica linear grating coated with dielectric materials via ALD.[109] Discrete layers of TiO_2 deposited by ALD serve as model analyte systems.[109]

The advantages of ALD mentioned in Section 2 indicate that it is suitable for bio-inspired research and designs. Conformal ALD was used by Summers et al. in 2010 to exploit biologically defined 2D photonic crystal templates of the *Papilio blumei* butterfly with the purpose of increasing the understanding of the optical effects of naturally formed dielectric architectures, and of exploring any novel optical effects.[36] This investigation demonstrated that faithful mimicry of *Papilio palinurus* can be achieved by physical fabrication methods through the use of breath figures to provide templates and ALD routines to enable optical properties.[36] Meanwhile, knowledge of the optical structure properties of the *Princeps nireus* butterfly has resulted in bio-inspired designs to enhance scintillator designs for radiation detection.[36] As ALD technology develops, more and more interesting optical microdevices will be fabricated.

4. Conclusions and Outlook

ALD offers special modification for optical devices. Research into the modification of optical properties is currently one of the most active development fields for ALD technology. While valuable progress has been made over the past 30+ years, we believe that the most significant advancements and impacts are still awaiting discovery and understanding. There are undoubtedly a large number of new potential applications emerging from fundamental research, especially concerning optical nano-/microdevices. Normally, new materials and functions introduced by the ALD process will lead to interesting new developments of optical nano-/microdevices in the next few years. Up-conversion luminescent materials, temperature sensitive materials, and others are excellent candidates for the discovery of novel functions of optical nano-/microdevices. Metamaterials are artificially designed sub wavelength composites possessing extraordinary optical properties, resulting in negative refraction, sub wavelength imaging, and cloaking.[110–112] For example, one porous alumina template was prepared by electrochemical anodization, into which silver nanowires were electrochemically deposited.[111] Obviously, due to its excellent advantages, ALD technology exhibits a great potential application for the fabrication of new metamaterials.

Received: October 8, 2013
Revised: March 19, 2014

[1] T. Suntola, J. Antson, US Patent 4058430 **1977**.
[2] M. Knez, K. Nielsch, L. Niinistö, *Adv. Mater.* **2007**, *19*, 3425.
[3] E. Graugnard, O. M. Roche, S. N. Dunham, J. S. King, D. N. Sharp, R. G. Denning, A. J. Turberfield, C. J. Summers, *Appl. Phys. Lett.* **2009**, *94*, 263109.
[4] I. Alessandri, M. Zucca, M. Ferroni, E. Bontempi, L. E. Depero, *Small* **2009**, *5*, 336.
[5] F. Kayaci, C. Ozgit-Akgun, I. Donmez, N. Biyikli, T. Uyar, *Acs. Appl. Mater. Interfaces* **2012**, *4*, 6185.
[6] F. B. Li, Y. Yang, Y. Q. Fan, W. H. Xing, Y. Wang, *J. Memb. Sci.* **2012**, *397*, 17.
[7] J. Dendooven, B. Goris, K. Devloo-Casier, E. Levrau, E. Biermans, M. R. Baklanov, K. F. Ludwig, P. Van der Voort, S. Bals, C. Detavernier, *Chem. Mater.* **2012**, *24*, 1992.
[8] X. B. Meng, X. Q. Yang, X. L. Sun, *Adv. Mater.* **2012**, *24*, 3589.
[9] J. Hamalainen, J. Holopainen, F. Munnik, T. Hatanpaa, M. Heikkila, M. Ritala, M. Leskela, *J. Electrochem. Soc.* **2012**, *159*, A259.
[10] M. Leskela, M. Ritala, *Thin Solid Films* **2002**, *409*, 138.
[11] D. Y. Moon, D. S. Han, J. H. Park, S. Y. Shin, J. W. Park, B. M. Kim, J. Y. Cho, *Thin Solid Films* **2012**, *521*, 146.
[12] G. Pardon, H. K. Gatty, G. Stemme, W. van der Wijngaart, N. Roxhed, *Nanotechnology* **2013**, *24*, 015602.
[13] C. J. Kirkpatrick, B. Lee, R. Suri, X. Y. Yang, V. Misra, *IEEE Electron Dev. Lett.* **2012**, *33*, 1240.
[14] K. Black, H. C. Aspinall, A. C. Jones, K. Przybylak, J. Bacsa, P. R. Chalker, S. Taylor, C. Z. Zhao, S. D. Elliott, A. Zydor, P. N. Heys, *J. Mater. Chem.* **2008**, *18*, 4561.
[15] E. Thimsen, S. C. Riha, S. V. Baryshev, A. B. F. Martinson, J. W. Elam, M. J. Pellin, *Chem. Mater.* **2012**, *24*, 3188.
[16] P. Sinsermsuksakul, J. Heo, W. Noh, A. S. Hock, R. G. Gordon, *Adv. Energy Mater.* **2011**, *1*, 1116.
[17] C. B. Zhang, L. Wielunski, B. G. Willis, *Appl. Surf. Sci.* **2011**, *257*, 4826.
[18] J. R. Bakke, J. T. Tanskanen, H. J. Jung, R. Sinclair, S. F. Bent, *J. Mater. Chem.* **2011**, *21*, 743.
[19] V. Brize, T. Prieur, P. Violet, L. Artaud, G. Berthome, E. Blanquet, R. Boichot, S. Coindeau, B. Doisneau, A. Farcy, A. Mantoux, I. Nuta, M. Pons, F. Volpi, *Chem. Vap. Deposition* **2011**, *17*, 284.
[20] S. Somani, A. Mukhopadhyay, C. Musgrave, *J. Phys. Chem. C* **2011**, *115*, 11507.
[21] H. Sen, J. Qimeng, Y. Shu, Z. Chunhua, K. J. Chen, *IEEE Electron Dev. Lett.* **2012**, *33*, 516.
[22] T. T. Van, J. P. Chang, *Appl. Phys. Lett.* **2005**, *87*, 011907.
[23] J. Hoang, T. T. Van, M. Sawkar-Mathur, B. Hoex, M. C. M. Van de Sanden, W. M. M. Kessels, R. Ostroumov, K. L. Wang, J. R. Bargar, J. P. Chang, *J. Appl. Phys.* **2007**, *101*, 123116.
[24] H. Kim, H. B. R. Lee, W. J. Maeng, *Thin Solid Films* **2009**, *517*, 2563.
[25] V. A. B. Quinones, G. S. Huang, J. D. Plumhof, S. Kiravittaya, A. Rastelli, Y. F. Mei, O. G. Schmidt, *Opt. Lett.* **2009**, *34*, 2354.
[26] E. J. Smith, W. Xi, D. Makarov, I. Monch, S. Harazim, V. A. B. Quinones, C. K. Schmidt, Y. F. Mei, S. Sanchez, O. G. Schmidt, *Lab Chip* **2012**, *12*, 1917.
[27] K. J. Vahala, *Nature* **2003**, *424*, 839.
[28] J. Wang, T. Zhan, G. Huang, P. K. Chu, Y. Mei, *Laser Photonics Rev.* **2013**.
[29] H. C. M. Knoops, M. E. Donders, M. C. M. van de Sanden, P. H. L. Notten, W. M. M. Kessels, *J. Vac. Sci. Technol. A* **2012**, *30*, 010801.
[30] J. Wang, T. R. Zhan, G. S. Huang, X. G. Cui, X. H. Hu, Y. F. Mei, *Opt. Express* **2012**, *20*, 18555.
[31] J. S. King, E. Graugnard, C. J. Summers, *Appl. Phys. Lett.* **2006**, *88*, 081109.
[32] T. Zhan, C. Xu, F. Zhao, Z. Xiong, X. Hu, G. Huang, Y. Mei, J. Zi, *Appl. Phys. Lett.* **2011**, *99*, 211104.
[33] P. F. Carcia, R. S. McLean, M. H. Reilly, M. D. Groner, S. M. George, *Appl. Phys. Lett.* **2006**, *89*, 031915.
[34] S. H. K. Park, J. Oh, C. S. Hwang, J. I. Lee, Y. S. Yang, H. Y. Chu, *Electrochem. Solid State Lett.* **2005**, *8*, H21.
[35] M. D. Groner, F. H. Fabreguette, J. W. Elam, S. M. George, *Chem. Mater.* **2004**, *16*, 639.

© 2014 WILEY-VCH Verlag GmbH & Co. KGaA, Weinheim

[36] C. J. Summers, D. P. Gaillot, M. Crne, J. Blair, J. O. Park, M. Srinivasarao, O. Deparis, V. Welch, J. P. Vigneron, *J. Nonlinear Opt. Phys. Mater.* **2010**, *19*, 489.
[37] M. Knez, A. Kadri, C. Wege, U. Gosele, H. Jeske, K. Nielsch, *Nano Lett.* **2006**, *6*, 1172.
[38] G. S. Huang, S. Kiravittaya, V. A. B. Quinones, F. Ding, M. Benyoucef, A. Rastelli, Y. F. Mei, O. G. Schmidt, *Appl. Phys. Lett.* **2009**, *94*, 141901.
[39] E. Graugnard, D. P. Gaillot, S. N. Dunham, C. W. Neff, T. Yamashita, C. J. Summers, *Appl. Phys. Lett.* **2006**, *89*, 181108.
[40] Z. A. Sechrist, F. H. Fabreguette, O. Heintz, T. M. Phung, D. C. Johnson, S. M. George, *Chem. Mater.* **2005**, *17*, 3475.
[41] J. K. Espoo, M. S. Leuven, US Patent 7067407 B2, **2005**.
[42] K. J. Russell, K. Y. M. Yeung, E. Hu, *Phys. Rev. B* **2012**, *85*, 245445.
[43] J. Zhao, Y. Wang, *J. Phys. Chem. C* **2012**, *116*, 11867.
[44] J. W. Elam, Z. A. Sechrist, S. M. George, *Thin Solid Films* **2002**, *414*, 43.
[45] G. Dingemans, A. Clark, J. A. van Delft, M. C. M. van de Sanden, W. M. M. Kessels, *J. Appl. Phys.* **2011**, *109*, 113107.
[46] S. Lange, V. Kiisk, V. Reedo, M. Kirm, J. Aarik, I. Sildos, *Opt. Mater.* **2006**, *28*, 1238.
[47] K. B. Klepper, O. Nilsen, H. Fjellvag, *Dalton Trans.* **2010**, *39*, 11628.
[48] V. V. Atuchin, V. N. Kruchinin, A. V. Kalinkin, V. S. Aliev, S. V. Rykhlitskii, V. A. Shvets, E. V. Spesivtsev, *Opt. Spectrosc.* **2009**, *106*, 72.
[49] C. L. Dezelah, J. Niinisto, K. Kukli, F. Munnik, J. Lu, M. Ritala, M. Leskela, L. Niinisto, *Chem. Vap. Deposition* **2008**, *14*, 358.
[50] T. S. Yang, K. S. An, E. J. Lee, W. Cho, H. S. Jang, S. K. Park, Y. K. Lee, T. M. Chung, C. G. Kim, S. Kim, J. H. Hwang, C. Lee, N. S. Lee, Y. Kim, *Chem. Mater.* **2005**, *17*, 6713.
[51] K. Kukli, M. Ritala, J. Lu, A. Harsta, M. Leskela, *J. Electrochem. Soc.* **2004**, *151*, F189.
[52] L. Dong, Q.-Q. Sun, Y. Shi, H. Liu, C. Wang, S.-J. Ding, D. W. Zhang, *Appl. Phys. Lett.* **2008**, *92*, 111105.
[53] I. M. Povey, D. Whitehead, K. Thomas, M. E. Pemble, M. Bardosova, J. Renard, *Appl. Phys. Lett.* **2006**, *89*, 104103.
[54] Z. Fang, H. C. Aspinall, R. Odedra, R. J. Potter, *J. Cryst. Growth* **2011**, *331*, 33.
[55] M. Ritala, P. Kalsi, D. Riihela, K. Kukli, M. Leskela, J. Jokinen, *Chem. Mater.* **1999**, *11*, 1712.
[56] K. E. Elers, T. Blomberg, M. Peussa, B. Aitchison, S. Haukka, S. Marcus, *Chem. Vap. Deposition* **2006**, *12*, 13.
[57] M. Ritala, M. Leskelä, J.-P. Dekker, C. Mutsaers, P. J. Soininen, J. Skarp, *Chem. Vap. Deposition* **1999**, *5*, 7.
[58] D. Gu, H. Baumgart, K. Tapily, P. Shrestha, G. Namkoong, X. Ao, F. Muller, *Nano Res.* **2011**, *4*, 164.
[59] D. Gu, H. Baumgart, T. M. Abdel-Fattah, G. Namkoong, *Acs Nano* **2010**, *4*, 753.
[60] D. J. Comstock, J. W. Elam, *Chem. Mater.* **2012**, *24*, 4011.
[61] F. B. Li, X. P. Yao, Z. G. Wang, W. H. Xing, W. Q. Jin, J. Huang, Y. Wang, *Nano Lett.* **2012**, *12*, 5033.
[62] Y. Qin, Y. Kim, L. Zhang, S.-M. Lee, R. B. Yang, A. Pan, K. Mathwig, M. Alexe, U. Gösele, M. Knez, *Small* **2010**, *6*, 910.
[63] M. S. Sander, M. J. Cote, W. Gu, B. M. Kile, C. P. Tripp, *Adv. Mater.* **2004**, *16*, 2052.
[64] L. Velleman, G. Triani, P. J. Evans, J. G. Shapter, D. Losic, *Microporus Mesoporus Mater.* **2009**, *126*, 87.
[65] J. W. Elam, D. Routkevitch, P. P. Mardilovich, S. M. George, *Chem. Mater.* **2003**, *15*, 3507.
[66] C. Marichy, M. Bechelany, N. Pinna, *Adv. Mater.* **2012**, *24*, 1017.
[67] A. Rugge, J. S. Becker, R. G. Gordon, S. H. Tolbert, *Nano Lett.* **2003**, *3*, 1293.
[68] X. D. Wang, C. Neff, E. Graugnard, Y. Ding, J. S. King, L. A. Pranger, R. Tannenbaum, Z. L. Wang, C. J. Summers, *Adv. Mater.* **2005**, *17*, 2103.
[69] J. S. King, E. Graugnard, O. M. Roche, D. N. Sharp, J. Scrimgeour, R. G. Denning, A. J. Turberfield, C. J. Summers, *Adv. Mater.* **2006**, *18*, 1561.
[70] J.-H. Lee, W. Leung, J. Ahn, T. Lee, I.-S. Park, K. Constant, H. Kai-Ming, *Appl. Phys. Lett.* **2007**, *90*, 151101.
[71] S. Kiravittaya, H. S. Lee, L. Balet, L. H. Li, M. Francardi, A. Gerardino, A. Fiore, A. Rastelli, O. G. Schmidt, *J. Appl. Phys.* **2011**, *109*, 053115.
[72] E. Graugnard, J. S. King, S. Jain, C. J. Summers, Y. Zhang-Williams, I. C. Khoo, *Phys. Rev. B* **2005**, *72*, 233105.
[73] J. S. King, E. Graugnard, C. J. Summers, *Adv. Mater.* **2005**, *17*, 1010.
[74] A. Rugge, J.-S. Park, R. G. Gordon, S. H. Tolbert, *J. Phys. Chem. B* **2004**, *109*, 3764.
[75] M. Scharrer, A. Yamilov, X. Wu, H. Cao, R. P. H. Chang, *Appl. Phys. Lett.* **2006**, *88*, 201103.
[76] M. Scharrer, X. Wu, A. Yamilov, H. Cao, R. P. H. Chang, *Appl. Phys. Lett.* **2005**, *86*, 151113.
[77] Z. A. Sechrist, B. T. Schwartz, J. H. Lee, J. A. McCormick, R. Piestun, W. Park, S. M. George, *Chem. Mater.* **2006**, *18*, 3562.
[78] E. Graugnard, J. S. King, D. P. Gaillot, C. J. Summers, *Adv. Funct. Mater.* **2006**, *16*, 1187.
[79] S. K. Karuturi, C. W. Cheng, L. J. Liu, L. T. Su, H. J. Fan, A. I. Y. Tok, *Nano Energy* **2012**, *1*, 322.
[80] C. W. Cheng, S. K. Karuturi, L. J. Liu, J. P. Liu, H. X. Li, L. T. Su, A. I. Y. Tok, H. J. Fan, *Small* **2012**, *8*, 37.
[81] L. T. Su, S. K. Karuturi, J. S. Luo, L. J. Liu, X. F. Liu, J. Guo, T. C. Sum, R. R. Deng, H. J. Fan, X. G. Liu, A. I. Y. Tok, *Adv. Mater.* **2013**, *25*, 1603.
[82] D. P. Gaillot, E. Graugnard, J. Blair, C. J. Summers, *Appl. Phys. Lett.* **2007**, *91*, 181123.
[83] H. K. Park, S. W. Yoon, D. Y. Choi, Y. R. Do, *J. Mater. Chem. C* **2013**, *1*, 1732.
[84] V. A. Bolans Quines, G. Huang, J. D. Plumhof, S. Kiravittaya, A. Rastelli, Y. Mei, O. G. Schmidt, *Opt. Lett.* **2009**, *34*, 2345.
[85] J. Zhong, J. Wang, G. Huang, G. Yuan, Y. Mei, *Nanoscale Res. Lett.* **2013**, *8*, 1.
[86] G. S. Huang, V. A. B. Quinones, F. Ding, S. Kiravittaya, Y. F. Mei, O. G. Schmidt, *ACS Nano* **2010**, *4*, 3123.
[87] E. J. Smith, S. Schulze, S. Kiravittaya, Y. F. Mei, S. Sanchez, O. G. Schmidt, *Nano Lett.* **2011**, *11*, 4037.
[88] G. S. Huang, Y. F. Mei, D. J. Thurmer, E. Coric, O. G. Schmidt, *Lab Chip* **2009**, *9*, 263.
[89] M. Yu, Y. Huang, J. Ballweg, H. Shin, M. Huang, D. E. Savage, M. G. Lagally, E. W. Dent, R. H. Blick, J. C. Williams, *ACS Nano* **2011**, *5*, 2447.
[90] S. M. Harazim, W. Xi, C. K. Schmidt, S. Sanchez, O. G. Schmidt, *J. Mater. Chem.* **2012**, *22*, 2878.
[91] M. L. Brongersma, V. M. Shalaev, *Science* **2010**, *328*, 440.
[92] A. Polman, *Science* **2008**, *322*, 868.
[93] S. Lal, S. Link, N. J. Halas, *Nat. Photonics* **2007**, *1*, 641.
[94] H. T. Miyazaki, Y. Kurokawa, *Phys. Rev. Lett.* **2006**, *96*, 097401.
[95] S. I. Bozhevolnyi, V. S. Volkov, E. Devaux, J.-Y. Laluet, T. W. Ebbesen, *Nature* **2006**, *440*, 508.
[96] H. Im, N. J. Wittenberg, N. C. Lindquist, S. H. Oh, *J. Mater. Res.* **2012**, *27*, 663.
[97] H. Im, K. C. Bantz, S. H. Lee, T. W. Johnson, C. L. Haynes, S.-H. Oh, *Adv. Mater.* **2013**, *25*, 2678.
[98] H. Im, K. C. Bantz, N. C. Lindquist, C. L. Haynes, S.-H. Oh, *Nano Lett.* **2010**, *10*, 2231.
[99] A. Polyakov, K. F. Thompson, S. D. Dhuey, D. L. Olynick, S. Cabrini, P. J. Schuck, H. A. Padmore, *Sci. Rep.* **2012**, *2*, 933.
[100] R. Raghavan, M. Bechelany, M. Parlinska, D. Frey, W. M. Mook, A. Beyer, J. Michler, I. Utke, *Appl. Phys. Lett.* **2012**, *100*, 191912.
[101] Y. S. Kim, S. Jin Yun, *J. Cryst. Growth* **2005**, *274*, 585.
[102] R. M. Costescu, D. G. Cahill, F. H. Fabreguette, Z. A. Sechrist, S. M. George, *Science* **2004**, *303*, 989.
[103] M. Barhoum, J. M. Morrill, D. Riassetto, M. H. Bartl, *Chem. Mater.* **2011**, *23*, 5177.
[104] N. T. Gabriel, J. J. Talghader, *Appl. Optics* **2010**, *49*, 1242.
[105] J. J. Wang, A. Nikolov, W. Qihong, *IEEE Photonic. Tech. Lett.* **2006**, *18*, 2650.
[106] M. R. Saleem, P. Stenberg, T. Alasaarela, P. Silfsten, M. B. Khan, S. Honkanen, J. Turunen, *Opt. Express* **2011**, *19*, 24241.
[107] T. Weber, T. Kasebier, A. Szeghalmi, M. Knez, E.-B. Kley, A. Tunnermann, *Nanoscale Res. Lett.* **2011**, *6*, 1.
[108] T. Alasaarela, D. Korn, L. Alloatti, A. Saynatjoki, A. Tervonen, R. Palmer, J. Leuthold, W. Freude, S. Honkanen, *Opt. Express* **2011**, *19*, 11529.
[109] A. Szeghalmi, E. B. Kley, M. Knez, *J. Phys. Chem. C* **2010**, *114*, 21150.
[110] Z. Liu, H. Lee, Y. Xiong, C. Sun, X. Zhang, *Science* **2007**, *315*, 1686.
[111] J. Yao, Z. Liu, Y. Liu, Y. Wang, C. Sun, G. Bartal, A. M. Stacy, X. Zhang, *Science* **2008**, *321*, 930.
[112] J. K. Gansel, M. Thiel, M. S. Rill, M. Decker, K. Bade, V. Saile, G. von Freymann, S. Linden, M. Wegener, *Science* **2009**, *325*, 1513.

 © 2014 WILEY-VCH Verlag GmbH & Co. KGaA, Weinheim